

EFFECT OF REBAR CORROSION ON THE BEHAVIOR OF A REINFORCED CONCRETE BEAM USING MODELING AND EXPERIMENTAL RESULTS

VPLIV KOROZIJE BETONSKEGA ŽELEZA NA ARMIRANOBETONSKI STEBER Z UPORABO MODELIRANJA IN EKSPERIMENTALNIH REZULTATOV

Ali Ghods, Mohammad Reza Sohrabi, Mahmoud Miri

University of Sistan and Baluchestan, Faculty of Engineering, Department of Civil Engineering, P.O. Box 9816745563-162, Zahedan, Iran
ali.ghods@pgs.usb.ac.ir

Prejem rokopisa – received: 2013-07-21; sprejem za objavo – accepted for publication: 2013-09-13

Reinforcement corrosion in concrete may cause adverse effects, such as the area reduction of rebars, concrete cracking, a reduction of the bond strength and a change in the bond-slip behavior between concrete and rebars. All these effects will finally lead to the inappropriate performance of concrete structures. In this paper a corroded reinforced concrete beam, whose experimental results are available, is modeled based on the finite-element method using ANSYS. The results are then compared with the available and confirmed results. A reduction of the reinforcement area and a change in the bond strength between the concrete and the reinforcement are seen in the model. The effect of reinforcement corrosion on the force-displacement curve and the modeled beam are also studied and compared with the results from reinforced concrete made in the laboratory. It was observed that with an increase of the reinforcement corrosion rate, the load-carrying capacity of the concrete beam and the bond strength decreases. In addition, the area under the load-displacement curve of the concrete beam decreases with the increase of the reinforcement corrosion.

Keywords: corrosion, beam, modeling, force-displacement

Korozija armature v betonu lahko vpliva škodljivo, tako kot zmanjšanje prereza betonskega železa, pokanje betona, zmanjšanje sile vezanja in sprememba vedenja vezave in drsenja med betonom in armaturo; vse to privede do neprimernih lastnosti betonske konstrukcije. V tem članku je bil modeliran z uporabo metode končnih elementov in ANSYS korodiran betonski steber s poznanimi eksperimentalnimi podatki. Rezultati so bili primerjani z razpoložljivimi in preverjenimi rezultati. Iz modela je razvidno zmanjšanje področja utrditve in sprememba v sili vezanja med betonom in armaturo. Preučevan je bil tudi vpliv korozije armature na krivuljo sila – raztezek in modeliran steber ter primerjan z laboratorijskimi rezultati pri armiranem betonu. Ugotovljeno je, da se z naraščanjem hitrosti korozije armature zmanjšujeta nosilnost betonskega stebra in sila vezanja. Področje pod krivuljo obremenitev – raztezek armiranega betonskega stebra se zmanjšuje z večanjem korozije armature.

Ključne besede: korozija, steber, modeliranje, sila – raztezek

1 INTRODUCTION

Reinforcement corrosion is one of the major factors in the deterioration of reinforced concrete structures, such as bridges, parking and coastal structures. This phenomenon may lead to area reduction of rebars, cracking, concrete scaling, reduction of bond strength and change in the bond-slip behavior between concrete and rebars. All of these factors will eventually lead to the adverse function of concrete structures.

The area reduction of rebars is the most evident result of rebar corrosion. Although carbonate corrosion in concrete occurs uniformly, chloride corrosion usually causes local corrosion known as 'pitting'.¹ It causes a considerable area reduction of rebars, which sometimes occurs without any noticeable signs.²⁻⁴

Some parts of the earlier literature focused on the bond reduction between concrete and rebar and its effect on the strength of beams and reinforced concrete slabs.^{5,6} In fact, the reduction of the bond strength between the concrete and the rebar occurs in two stages. During the early stage, corrosion products gather on the rebar surface and increase its diameter. This phenomenon increases the radial stresses between the concrete and the

rebar, which intensifies the factor of cohesive friction.⁴ During the next stage, longitudinal cracks reduce the confinement of corrosion products, which in turn reduces the bond strength. The more the corrosion proceeds, the more the bond-strength reduction will emerge.

Similar to any other engineering issue, studies concerning corrosion were conducted through three general methods, including experimental, analytical, and numerical simulation. A few studies have been carried out using numerical studies and applying some known finite-element software aiming to study the effects of reinforcement corrosion in concrete. For instance, Berra et al.⁷ investigated the effect of corrosion on the bond deterioration between concrete and rebar using ABAQUS. Lundgren⁸ used DIANA finite-element software for the numerical simulation of the experimental creation of cracks, caused by corrosion, and corroded rebar pullout tests. Saether and Sand⁹ also modeled a corroded reinforced concrete beam, for which the experimental results were available. Meanwhile, they used DIANA and obtained similar results with the created sample. Most of the earlier finite-element models were two-dimensional.¹⁰ An attempt is made in the current research to present a 3D model using ANSYS for a beam, for which

the experimental results are available. The results obtained from the finite-element analysis of this beam are compared with the available ones. After verification of the model, a parametric study is carried out on the beam. It means that the load-displacement curve is drawn at different percentages of the corrosion and variations in the load-carrying capacity of the beam are studied. They are then compared with the load-displacement curve of the beams made in the laboratory. Finally, the reinforcement slip in the concrete is studied for various percentages of the corrosion using the model.

2 ELEMENTS USED IN ANSYS

2.1 Element for concrete

The SOLID65 element is a 3D element with eight nodes and three degrees of freedom (translation on x , y , z directions) in each node. The element is capable of modeling the fissures and breaks of concrete.^{11,12} A major aspect of the element is the nonlinear performance of its materials. Reinforcement can be defined in this element as well; of course, the reinforcements are defined individually here. Multi-linear isotropic hardening under the von Mises fracture criteria is used in this element. Generally, five coefficients are used to determine its smooth break, which include one-axis tensile strength, one-axis compressive strength, two-axis compressive strength, and one- and two-axis compressive strength under a specific confining pressure. Moreover, the shear transmission coefficients can also be applied as the inputs for open and close cracks. **Figure 1** exhibits the geometrical specifications of the SOLID65 element.

2.2 Element for Reinforcement

All the tensional and compressive reinforcements and stirrups are modeled in this study using the LINK8 ele-

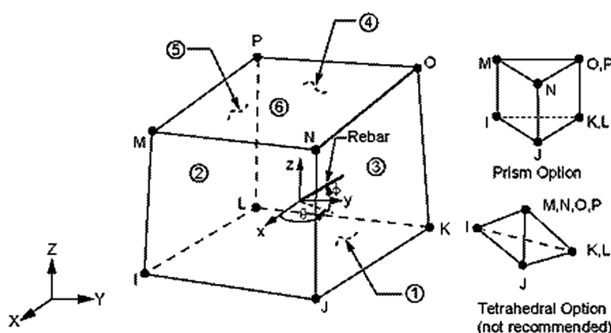


Figure 1: Geometry and specifications of the SOLID65 element
Slika 1: Geometrija in podrobnosti elementa SOLID65

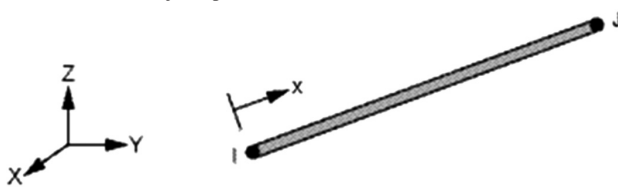


Figure 2: Geometry and specifications of the LINK8 element
Slika 2: Geometrija in podrobnosti elementa LINK8

ment. This element is a 3D element, only with tensional and/or compressive axial forces.^{11,12} The element has two nodes with three degrees of freedom in each node, including translation for the x , y , z directions. The input of this element is the cross-section. **Figure 2** presents the specifications for this element.

2.3 Element for cohesion

The COMBIN39 element is applied for modeling the cohesion between the concrete and the rebar. This element is a uni-directional element capable of determining the force-displacement nonlinearity equation.^{11,13} In addition, it has axial and torsional capability in one-, two- and three-dimensional analyses. Its axial option, which is used here, has a maximum of three degrees of freedom in each node. This element can have zero length, i.e., the start and end nodes can be defined as on each other. **Figure 3** exhibits a sample of the load-displacement diagram of the element.

3 CONTROL BEAM OF MODELING

3.1 The Beam Tested by Rodriguez et al.

Here, we discuss one of the reinforced concrete beams with corroded rebars tested by Rodriguez et al.¹⁴ The test series of Rodriguez et al.¹⁴ include 31 beams with various details of reinforcement, different shear reinforcement and a range of corrosion percentages. **Figure 4** shows the geometry and specifications of the beam reinforcement for modeling in this paper.

As shown in the figure, this beam has both tensional and compressive reinforcement and stirrups. In the beams tested by Rodriguez et al.,¹⁴ the concrete had a compressive strength of between 48 MPa and 55 MPa. In order to accelerate the corrosion in the rebars, 3 % of calcium chloride (by mass of cement) was added to the concrete mix design. A compressive strength ranging from 31 MPa to 37 MPa was recorded for the concrete with the calcium chloride. The beams were cured under humid conditions for 28 d. Then a current of about 0.1 mA/cm² was applied to create an accelerated corrosion during the aging of the specimens, ranging from 100 d to 200 d.

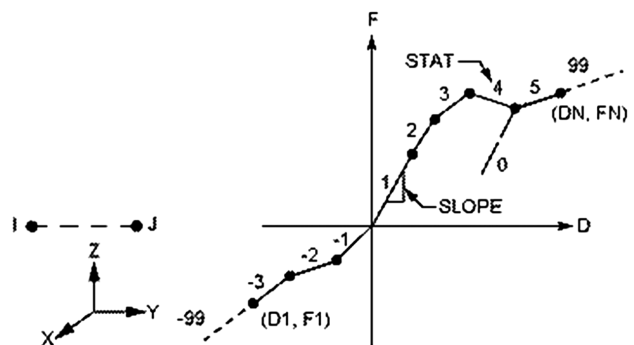


Figure 3: Geometry and specifications of the COMBIN39 element
Slika 3: Geometrija in podrobnosti elementa COMBIN39

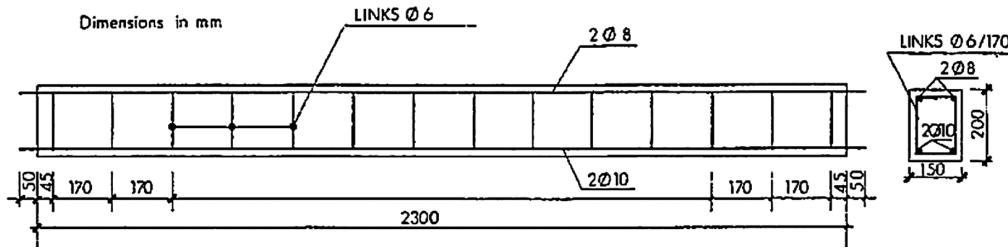


Figure 4: Geometry and specifications of the beam for modeling¹⁴
 Slika 4: Geometrija in podrobnosti stebra za modeliranje¹⁴

It should be noted that due to the presence of stirrups, the corrosion was not uniformly distributed along the longitudinal rebars and the corrosion rate for the tensional and compressive rebars and stirrups was different in each beam. After the completion of the accelerated corrosion process, the beams were exposed to a four-point bending test. Table 1 lists the complete characteristics of the beams for modeling. The non-corroded and corroded beams tested by Rodriguez et al.¹⁴ are shown by Rod.01 and Rod.02 respectively in the remainder of the paper

Table 1: Specifications of the beams for modeling¹⁴
 Tabela 1: Podrobnosti za modeliranje stebra¹⁴

Parameter			Beam with Corrosion	Beam without Corrosion
			Rod.02	Rod.01
One-axis compressive strength of concrete		f_c /MPa	31.4	50
One-axis tensile strength		f_t /MPa	2.8	3.5
Percentage of reinforcement		ρ %	0.5	0.5
Concrete elasticity modulus		E_c /MPa	28300	32200
Steel elasticity modulus		E_s /GPa	206	206
Steel elastoplastic tangent modulus		E_{st} /MPa	824	824
Tensile steel	Area reduction	%	13.9	–
Compressive steel	percentage due to corrosion	%	12.58	–
Stirrup		(%)	23.15	–

4 LABORATORY-MADE REINFORCED CONCRETE BEAM

Six reinforced concrete beams were made by the authors, using the same dimensions and reinforcement conditions as used by Rodriguez et al.¹⁴ Three beams were tested for a further validation of the modeled beam and evaluating the effect of the corrosion on the behavior of the reinforced concrete under test. A concrete mixer was used for concreting and the modularity of the beams. In addition, after pouring the concrete into the mold, it was compacted using a 1.5 cm diameter rod. The beams were extracted from the mold after 24 h and cured using sacks for 28 d. Two-layer pressure-resistance and humidity-resistance string wires were used to create an

electric current and to measure the corrosion in the concrete. The ends of the wires were taken out of the concrete. To protect the wires from corrosion and humidity, their ends were covered by an appropriated cohesive material before conducting the test. After 28 d of curing, the beam was placed in a distilled water basin containing 3 % of calcium chloride (by mass of distilled water). Then a negative current was applied in the basin to analyze salt to chlorine. To create the corrosion, a maximum 100 mA/cm² DC current was applied using wires. The other conditions are almost the same as those mentioned for the Rod.02 beam in Table 1. Hereinafter, these specimens are shown by Gh.03. Figure 5 shows an image of these samples.

5 MODELING OF BEAMS BY CORROSION

5.1 Reinforcement Model

Uniform corrosion does not have a considerable effect on the stress-strain properties of the reinforcements and it is convenient to model it by reducing the cross-section of the steel rebars. Pitting corrosion may cause a significant reduction in the mechanical behavior of the steel reinforcement due to the local concentration of stress. Generally, if a reinforcement rebar initially has a diameter of φ_0 , its diameter will be reduced due to the corrosion. The remaining cross-section of the tension rebar affected by uniform corrosion can be calculated from Eq. (1):⁹

$$A_{res} = \frac{\pi\varphi_R^2}{4} = \frac{\pi(\varphi_0 - \alpha x)^2}{4} \quad (1)$$

Where φ_R is the remaining diameter of the reinforcement, α is a coefficient dependent on the type of corrosion and x shows the penetration rate of the corrosion.⁹



Figure 5: Reinforced concrete beams made by the authors (Gh.03)
 Slika 5: Armiranobetonski steber, ki so ga izdelali avtorji (Gh.03)

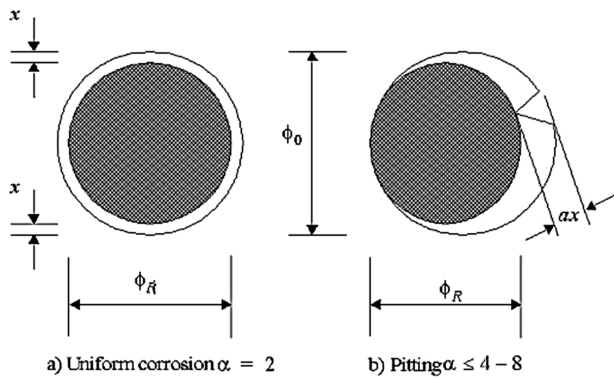


Figure 6: Remaining cross-section of the corroded rebar
Slika 6: Preostali prevez korodiranih palic v armaturi

For uniform corrosion it is assumed that the coefficient α is equal to 2. For pitting corrosion the cross-section becomes irregular and the area reduction may be considerably greater than the uniform corrosion (Figure 6). The above relation can be used for estimating the reinforcement cross-section in the pitting corrosion by introducing the circular cross-sectional diameter as φ_R . In this condition, the α coefficient is considered within the range of 4 to 8.⁹

In this study it is assumed that the corrosion is uniform. Therefore, no reduction is considered for the mechanical properties of the steel and only the area reduction is considered for the corroded reinforcements in the calculations. The stress-strain relation of the steel, in tension, was considered as an elastoplastic material with a linear hardening, which is shown in Figure 7.

5.2 Concrete Model

Cracked concrete, due to the corrosion under the effect of compressive stresses, shows a lower performance when compared with the un-cracked concrete. In this condition, the reduced compressive strength is used for the beams whose compression rebars are affected by corrosion. The amount of reduced compressive strength is suggested by Eq. (2):¹⁵

$$f_c^D = \frac{f_c}{\left[1+k\left(\frac{\epsilon_1}{\epsilon_{co}}\right)\right]} \tag{2}$$

In this equation, f_c^D is the compressive strength of the cracked concrete, f_c is the specified compressive strength of the un-cracked concrete, k is a coefficient equal to 0.1 ($k = 0.1$), ϵ_{co} is the strain of the concrete under the maximum load, and ϵ_1 is the lateral strain caused by the crack, which is a function of the corroded reinforcements number, the volume expansion of the corrosion products on the rebar, and the average amount of corrosion influence.

In modeling reinforcement beam by ANSYS, it is necessary to define the stress-strain curve for concrete. This relation depends on several factors. The most common forms are used here. One simple model to introduce a concrete stress-strain relation is the application of an idealized elastoplastic relation, which is shown in Figure 8a. Another model, which is more realistic, is the parabolic model, like that shown in Figure 8b. In both models, the tensional behavior of the concrete is shown by a two-linear estimation in which the tensile stress increases up to the tensile strength f_t and then it is followed by a softening behavior.

5.3 Bonding Model

Before the development of cracks in the concrete, low rates of corrosion may increase the bond strength between the reinforcement and the concrete. The bond strength starts decreasing with the formation of corrosive cracks, which normally occur along the reinforcement. There are numerous experimental results on corrosive reinforcements. However, the presence and development of corrosion products were proved to be the main parameter in weakening the bond strength between the corroded reinforcement and the concrete. Various relations have been offered for the bond strength. In the present study, the following relation is used for the bond strength. This relation considers the effects of both the concrete and the stirrups:¹⁶

$$u_{max}^D = R \cdot \left[0.55 + 0.24 \left(\frac{c}{d_b}\right)\right] \sqrt{f_c} + 0.191 \left(\frac{A_{st} f_{yt}}{s_s d_b}\right) \tag{3}$$

$$R = A_1 + A_2 X$$

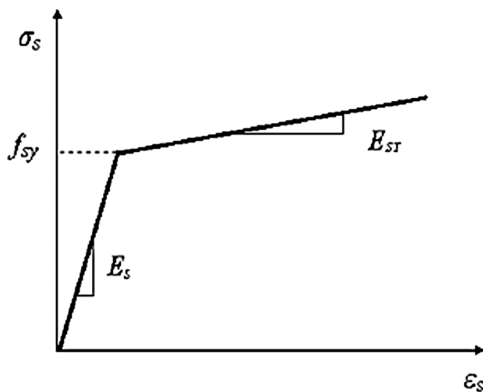


Figure 7: Stress-strain curve for rebars in tension
Slika 7: Krivulja napetost – raztezek pri natezni obremenitvi palice iz armature

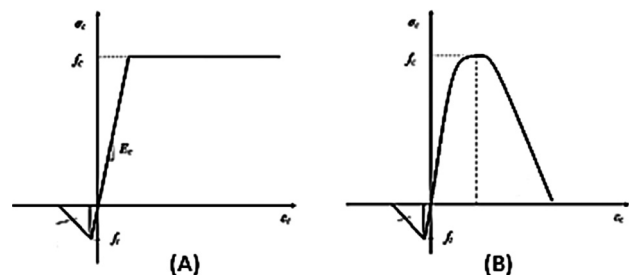


Figure 8: Different types of stress-strain curves for concrete
Slika 8: Različne krivulje napetost – raztezek za beton

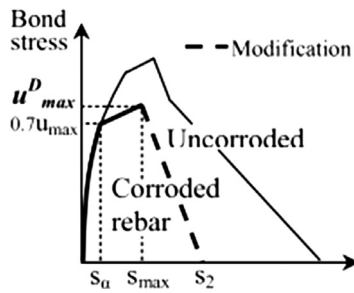


Figure 9: Diagram of the relation proposed for the bond-slip strength¹⁷

Slika 9: Diagram predlagane odvisnosti trdnosti za vezavo – drsenje¹⁷

Where u_{max}^D is the reduced bond strength, c is the thickness of concrete cover, d_b is the reinforcement diameter, f_c is the specified compressive strength of concrete, A_{st} is the area of shear reinforcement, f_{yt} is the yield strength of the stirrups, s_s is the stirrup spacing, and R is a factor that considers the reduction of the bond strength in which A_1 and A_2 are coefficients reflecting the rate of corrosion in an accelerated corrosion process. For corrosion process of 0.09 mA/cm², the values of these coefficients were determined as $A_1 = 1.104$, $A_2 = -0.024$. Finally, X is the corrosion rate, which is stated as a percentage of the rebar mass loss.

The advantage of this model for the bond strength between the concrete and the rebar is that it is capable of modeling the increase of the bond strength at low rates of corrosion. Obviously, this depends on the corrosion rate.

Studies show that the relation between the bond strength and the slip is controlled by the corrosion rate in longitudinal rebars and the rate of corrosion products. A modified relation was proposed for bond-slip rule by Harajli et al.,¹⁷ which is shown in Figure 9.

In this diagram $S_2 = 0.35c_0$, where c_0 is the distance between the rebar ribs, which is assumed to be 8 mm. Other specifications of the diagram are defined in the following relations:¹⁷

$$u = u_1 \left(\frac{s}{s_1} \right)^{0.3} \quad (4)$$

$$s_\alpha = s_1 \left(\frac{\alpha u_{max}^D}{u_1} \right)^{1/0.3} \quad (5)$$

$$s_{max} = s_1 e^{(1/0.3) \ln(u_{max}^D/u_1)} + s_0 \ln \left(\frac{u_1}{u_{max}^D} \right) \quad (6)$$

In these relations $S_1 = 0.15C_0$, $u_1 = 2.57(f_c)^{0.5}$, $\alpha = 0.7$, and the s_0 for plain and steel-reinforced concrete is 0.15 and 0.4, respectively.¹⁷

In this research the above diagram is used for modeling the bond stress between concrete and rebar. Of course, the element applied for bond modeling is COMBIN39. As explained in Section 2, this element needs a force-displacement curve. Therefore, the following equation is introduced for this purpose:¹⁷

$$F(s) = u(s)\pi dl \quad (7)$$

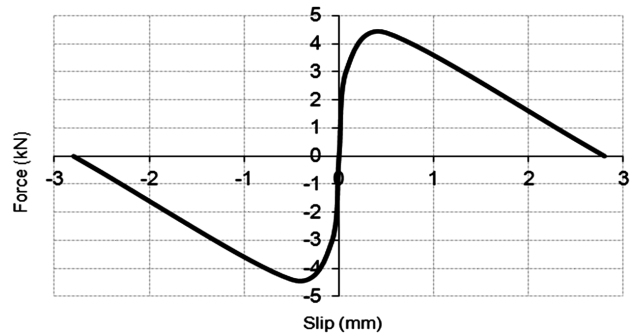


Figure 10: Force-slip diagram for the COMBIN39 element where the tension reinforcements are located

Slika 10: Diagram sila – zdrsa za element COMBIN39 pri natezni obremenitvi armature

In this relation, $F(s)$ is the shear force between the reinforcement and the concrete, $u(s)$ is the bond strength, d is the reinforcement diameter, and l is the distance between two adjacent COMBIN39 elements (Figure 10).

For instance, the relation between the force-slip for the corroded tension reinforcements is as follows, which is in fact the same force-slip diagram of COMBIN39 element where the tension reinforcements are located.

This diagram is obtained assuming a reduction of the reinforcement mass by 10 percent ($x = 10\%$). The corresponding force-slip diagrams for different percentages of reduction of the reinforcement mass are shown in Figure 11.

5.4 The Model Created using ANSYS

As explained in the earlier sections, a finite-element model of the control beam tested by Rodriguez et al.¹⁴ was made using ANSYS (Figure 12).

Because of the symmetrical condition, half of the beam was considered during modeling. It should be noted that it is a complicated task to make a precise model for a corroded reinforced beam. This is due to the fact that the corrosion rate along longitudinal rebars, caused by stirrups, is not constant. In addition, the average rate of corrosion in each beam for tensile and com-

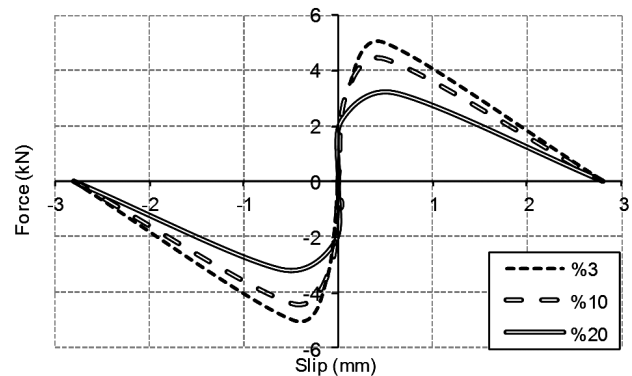


Figure 11: Force-slip diagram for COMBIN39 for different percentages of corrosion

Slika 11: Diagram sila – zdrsa za element COMBIN39 pri različnih deležih korozije

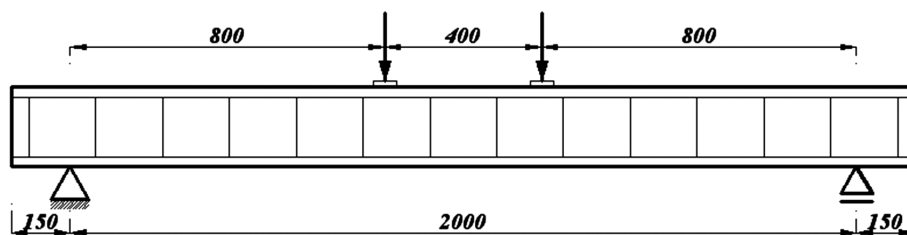


Figure 12: Supports and loading conditions for the control beam
 Slika 12: Podpore in obremenitev kontrolnega stebra

pressive reinforcements and stirrups is different. However, in the beam selected for modeling, the average rates of corrosion in the tensile and compressive reinforcements are almost equal.¹⁴ As shown in Table 1, the rates of corrosion in tensile and compressive reinforcements are 13.9 % and 12.6 %, respectively. It is noteworthy that in the finite-element model made here, changes to the reinforcement area were considered as mentioned in Section 1-4 and the changes of the bond stress were taken in to account, according to the remarks of Section 3-4 (Figures 13 and 14).

Finally, the load was applied to the model incrementally. Attempts were made to choose smaller incremental steps of load to obtain a better convergence. The load could be increased as long as it was not possible to increase it any more due to the model instability, using the Newton-Raphson method for the non-linear analysis.

In order to observe the sensitivity of the meshing size as a result of the existing model it is also investigated with mesh seeds of 100, 200 and 300 in each direction. After that the results were compared and it has clear that the differences were negligible; therefore, a mesh size of

100 was used in the ANSYS because of the speed and comfort.

6 MODELED BEAM RESULTS vs. EXPERIMENTAL RESULTS

Here, we continue the discussion by comparing the load-displacement curve at the mid-span of the modeled and the experimental beam. Figure 15 compares the results of the numerical analysis of the corrosion-free Rod.01 modeled beam with its experimental results. It is clear that the numerical modeling has a favorable precision, especially for estimating the factored load.

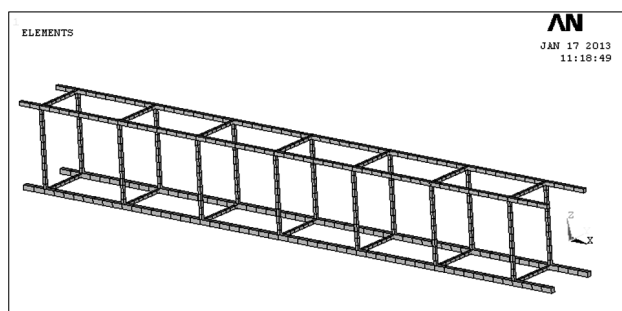


Figure 13: Modeled reinforcements
 Slika 13: Modelirana armaturna mreža

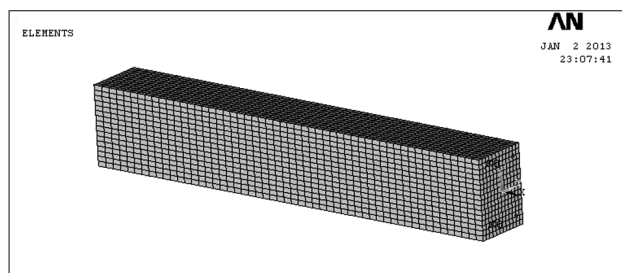


Figure 14: Control beam model on ANSYS
 Slika 14: ANSYS-model kontrolnega stebra

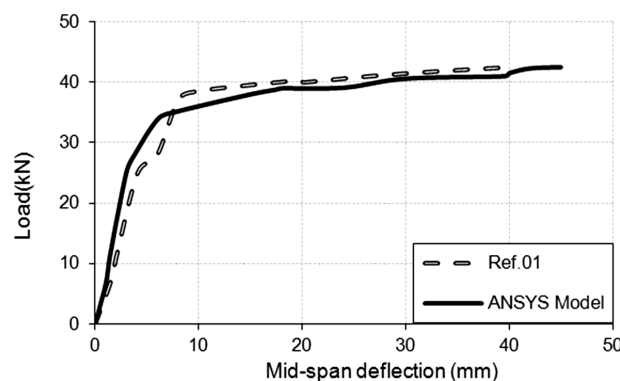


Figure 15: Numerical and experimental results of the load-displacement curves for the Rod.01 beam

Slika 15: Numerični in eksperimentalni rezultati obtežbe – raztežka pri stebru Rod.01

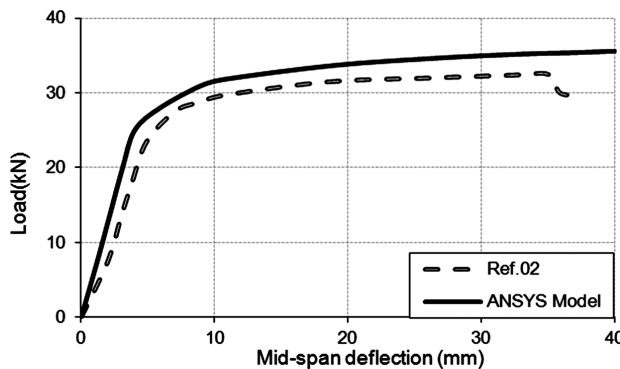


Figure 16: Numerical and experimental results of load-displacement curves for the Rod.02 beam (with corrosion)

Slika 16: Numerični in eksperimentalni rezultati obtežbe – raztežka pri stebru Rod.02 (s korozijo)

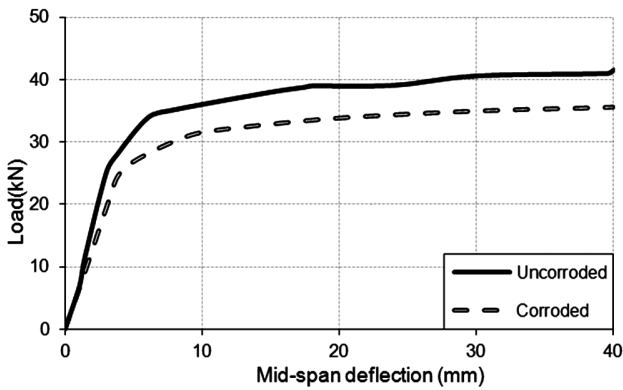


Figure 17: Numerical results of the load-displacement for the corroded and non-corroded model beam
Slika 17: Numerični rezultati obtežbe – raztezka za modelni steber s korozijo in brez nje

Figure 16 also shows the mid-span load-displacement relationships for the Rod.02 modeled beam and its experimental results, which are affected by the reinforcement corrosion. Comparing the results indicates a favorable precision between the results of the modeled beam by the authors and Rodriguez’s experimental results. The corroded beam in the model estimates the factored load with an error close to 9 % more than the Rod.02 beam. With respect to the specific complexities of the model and the approximations used in modeling, the numerical result has a favorable precision.

Figure 17 shows the results of the load-displacement for the corroded and non-corroded beams, obtained from the modeling, in a diagram.

It should be noted that the finite-element model underestimates the results of the non-corroded beam and overestimates the results of the corroded beam. Therefore, the difference of the load-carrying capacity between the corroded and non-corroded beams is underestimated as compared with the experimental results.

The results of the load-carrying capacity at different percentages of corrosion for the modeled beams and those created by the authors (Gh.03) are explained subsequently. Four-point loading is used, as shown in **Figure 18**, to achieve the load-carrying capacity of the beams in the laboratory. It should be noted that the parameter here introduced as an index to show the corrosion

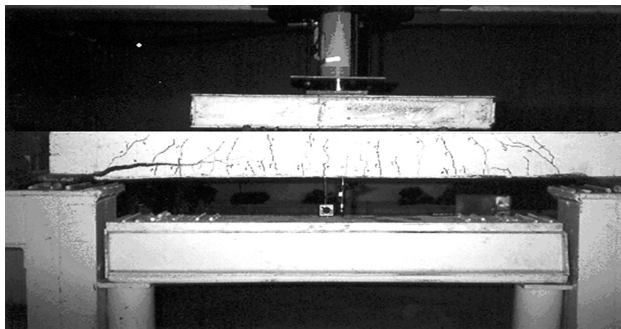


Figure 18: Four-point loading for corroded beam
Slika 18: Štiritočkovna obremenitev stebra s korozijo

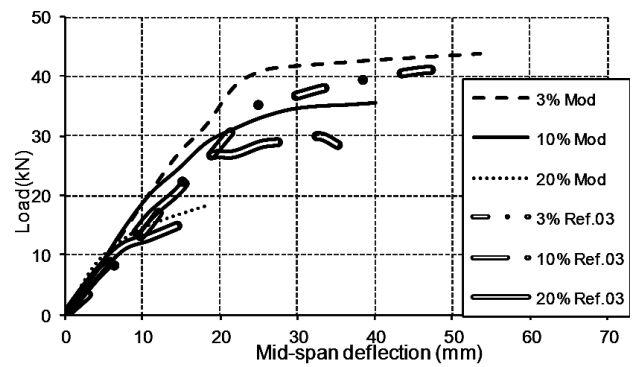


Figure 19: Results of load-displacement for different rates of corrosion in the model beam and Gh.03
Slika 19: Rezultati obtežbe – raztezka pri različnih stopnjah korozije pri modelnem stebru Gh.03

rate has the same percentage of mass for the reinforcements earlier introduced as the parameter x in the previous sections. **Figure 19** shows the amounts of load-displacement in (3, 10, and 20) % corrosion in the created beams (Gh.03) and the modeled beams.

Figure 19 shows that the increase of the corrosion rate reduces the ultimate load-carrying capacity and the ultimate displacement. In addition, the length of the non-linear area in the beam increases with lower rates of corrosion. Failure of the beams with a high rate of reinforcement corrosion will probably tend to approach a brittle fracture; of course, such a question requires a separate study. It means that their fracture mechanism can be studied through examining the formation of cracks and their positions at the time of the beam fracture with different rates of corrosion. The very good precision of the offered model can be observed by examining the results obtained from the force-displacement curve in the modeled and experimental beams. The differences among the precisions may be due to the variations in the rate of corrosion along the longitudinal rebars related to the existence of stirrups. In this figure, the results of the numerical analysis of the model are overestimated as compared with the experimental ones.

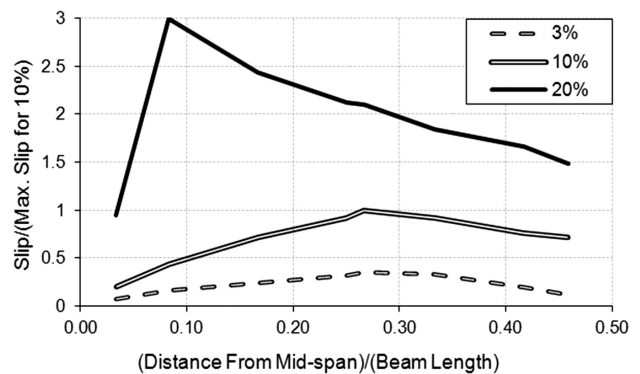


Figure 20: Rate of reinforcement slip in proportion to concrete for different rates of corrosion

Slika 20: Razmerje drsenja armature in betona pri različnih stopnjah korozije

With respect to the favorable precision of the modeled beam, the rate of reinforcement slip in proportion to concrete can be studied. In fact, it is the same displacement in the nonlinear spring element, which is placed for modeling the bonding strength between the concrete and the reinforcement. **Figure 20** shows the rate of reinforcement slip in proportion to the concrete along the beam. The diagram is drawn for different rates of corrosions.

The figure shows that the rate of slip increases with the increase of the rate of corrosion in the reinforcement. In fact, according to **Figure 11**, with an increase of the rate of corrosion, the concrete-reinforcement bond strength decreases. This leads to an increase of the slip. As **Figure 20** shows, the place with maximum slip in a beam with 20 % corrosion approaches the center of the beam.

7 CONCLUSION

A reinforced concrete beam with reinforcement corrosion was modeled in this paper. The area reduction of the reinforcement and the bond-strength reduction was observed between the concrete and the reinforcement. The results obtained from the finite-element analysis of this beam were compared with those achieved by Rodriguez.¹⁴ It was shown that there was a good agreement between the load-displacement diagram and the experimental work.

The reinforcement corrosion rate in the model was altered as a parameter, and its effect on the load-carrying capacity was studied. The results were then compared with those experienced by the authors.

It was revealed that with an increase of the reinforcement corrosion rate, the load-carrying capacity of the concrete beam decreases.

The area under the load-displacement curve of the concrete beam decreases with the increase of the reinforcement corrosion. This may be an indication for the reduction of the concrete beam's ductility. Therefore, it can be expected that the concrete beam will become more brittle with an increase of the corrosion.

By comparing the results obtained from the model with the beams made by the authors, very good precision of the model is realized. The difference may be due to the lack of uniform corrosion of the longitudinal rebars caused by stirrups, and the use of different methods for accelerating the corrosion by the authors and Rodriguez et al.¹⁴

It was observed that the bond strength reduces with an increase of the corrosion rate. This leads to an increase of reinforcement slip in reinforced concrete beams.

8 REFERENCES

- ¹ A. Kocijan, M. Jenko, Inhibition of the pitting corrosion of Grey cast Iron using carbonate, *Mater. Tehnol.*, 40 (2006) 1, 3–6
- ² A. R. Boga, Ý. B. Topçu, M. Öztürk, Effect of Fly-Ash amount and Cement type on the corrosion performance of the steel embedded in concrete, *Mater. Tehnol.*, 46 (2012) 5, 511–518
- ³ J. Cairns, Consequences of reinforcement corrosion for residual strength of deteriorating concrete structures, Proc. of the First Inter. Conference on Behavior of Damaged Structures, Rio de Janeiro, 1998
- ⁴ CEB Task Group 2.5, Bond of Reinforcement in Concrete, State-of-the-art report, fib Bulletin No. 10, 2000
- ⁵ L. Chung, H. Najm, P. Balaguru, Flexural behavior of concrete slabs with corroded bars, *Cement and Concrete Composites*, 30 (2008), 184–193
- ⁶ K. Toongoenthong, K. Maekawa, Multi-mechanical approach to structural assessment of corroded RC members in shear, *J. Advanced Concrete Technology*, 3 (2005) 1, 107–122
- ⁷ M. Berra, A. Castellani, D. Coronelli, S. Zanni, G. Zhang, Steel-concrete bond deterioration due to corrosion: finite-element analysis for different confinement levels, *Magazine of Concrete Research*, 55 (2003) 3, 237–247
- ⁸ K. Lundgren, Bond between ribbed bars and concrete Part I: Modified model, *Magazine of Concrete Research*, 57 (2005) 7, 371–382
- ⁹ I. Saether, B. Sand, FEM simulation of reinforced concrete beams attacked by corrosion, *ACI Structural J.*, 39 (2009) 3, 15–31
- ¹⁰ K. Narmashiri, M. Z. Jumaat, Reinforced steel I-beams: A comparison between 2D and 3D simulation, *Simulation Modelling Practice and Theory*, 19 (2011) 1, 564–585
- ¹¹ Ansys 11, Help Manual, 2011
- ¹² M. L. Bennegadi, Z. Sereir, S. Amziane, 3D nonlinear finite element model for the volume optimization of a RC beam externally reinforced with a HFRP plate, *Construction and Building Materials*, 38 (2013), 1152–1160
- ¹³ A. Pozolo, B. Andrawes, Analytical prediction of transfer length in prestressed self-consolidating concrete girders using pull-out test results, *Construction and Building Materials*, 25 (2011) 2, 1026–1036
- ¹⁴ J. Rodriguez, L. M. Ortega, J. Casal, J. M. Diez, Assessing structural conditions of concrete structures with corroded reinforcement, In: R. K. Dhir, M. R. Jones (editors), *Concrete repair, rehabilitation and protection*, E&FN Spon, 1996, 65–78
- ¹⁵ D. Coronelli, P. Gambarova, Structural assessment of corroded reinforced concrete beams: modelling guidelines, *J. Structural Engineering*, 130 (2004) 8, 1214–1224
- ¹⁶ T. E. Maaddawy, K. Soudki, T. Topper, Analytical model to predict nonlinear flexural behaviour of corroded reinforced concrete beams, *ACI Structural J.*, 102 (2005) 4, 550–559
- ¹⁷ M. H. Harajli, B. S. Hamad, A. A. Rteil, Effect of confinement on bond strength between steel bars and concrete, *ACI Structural J.*, 101 (2004) 5, 595–603